Thermal Performance Study Of A Prototype Multiport Heat Exchanger

Subhra Kanti Batabyal [(1)], Sohail Bux [(2)]
(1) Student(M.Tech), (2) H.O.D (Mechanical)
(1) (2) Ram Krishna Dharmarth Foundtion University, Gandhi Nagar, Bhopal, Madhya Pradesh, INDIA- 462033

Abstract: Great efforts have been made to investigate the thermal performance and fluid flow behaviour in Minichannel Heat Exchangers (MICHX), however, the examination of air side in a multiport serpentine slab heat exchanger is rare. In the current investigation, experiments were conducted on air heating via a prototype multiport MICHX. Hot DI water at different mass flow rates and a constant inlet temperature of 70°C was passed through the channels. The water sides Reynolds numbers were varied from 255 to 411. The airside Reynolds numbers were calculated based on the free mean stream velocity and varied from 1750 to 5250, while, the air inlet temperatures were in the range of 22.5°C to 34.5°C. The effects of dimensional parameters, such as Reynolds number, Nusselt number, Prandtl number, Brinkman number, and Dean number on the heat transfer performance were investigated. The effect of the serpentine on the enhancement of DI water thermal performance behaviour was studied. Heat transfer correlations were established and compared to the results in the open literature. The objective of the present study is to investigate the heat transfer characteristics of heating the air-side and cooling the liquid-side of a serpentine slab minichannel heat exchanger. The investigation determines the effect of the serpentine bend, the presence of the axial heat conduction, and viscous dissipation in the MICHX. The heat transfer correlation found from this current study is compared to the other available correlations.

NOMENCLATURE

A	Area (m^2)
A_a	Airside total heat transfer area (m^2)
Ac	Channel cross sectional area (m^2)
A_f	Fin surface area (m^2)
$A_{a.min}$	Airside minimum free flow area (m^2)
A_s	Heat transfer surface area (m^2)
B_r	Brinkman number
De	Dean number
D_{ha}	Airside hydraulic diameter (m)
D_{hw}	Water side hydraulic diameter (m)
Di	Channel inside diameter
Do	Channel outside diameter
Ec	Eckert number
F	LMTD correction factor for cross-flow and multi pass heat exchanger
L	Flow length (m)
L_{th}	Thermal entrance length
L_{hy}	Hydrodynamic entrance length
M	Axial conduction number
m	Fin parameter
MICHX	Minichannel heat exchanger
NTU	Number of transfer unit
P	Pressure (pa)
$\dot{Q}$	Heat transfer rate (w)
R	Radius of serpentine curvature
Re	Reynolds number
T	Temperature (°C)
Vi	Viscous dissipation number

I. INTRODUCTION

Energy exists in several forms such as heat, kinetic, mechanical, potential, electrical, etc. According to the law of conservation of energy, the total energy of a system remains constant, however, it may transform into different forms. The United States Energy Information Administration reported that the world's electrical demand will increase by almost 50% from the year of 2007 to 2035 in its International Energy Outlook (IEO), U.S. Energy Information Administration (2010).

While the actual rate at which population and electrical demands will increase is a point for debate, the idea that they will definitely be raised is widely agreed upon. A boost in electrical demand will result from such a population growth, which will require new power sources that are recently not under development.

A heat exchanger is a device used to facilitate the transfer of heat from one fluid to another without a direct contact between the fluids. Heat exchangers generally maximize the transfer of heat by increasing the contact surface area between the fluids. A conventional heat exchanger has an area density of 700 m^2/ m3, while the MICHX are density is in the order of about 5000 m^2/ m^3.

Air to water cross flow heat exchangers that consist of flow passes of various shapes have been frequently used in many applications. Therefore, a proper choice of the air and water side heat transfer correlations in the relevant design and applications is essential. To design such heat exchangers, some basic parameters have to be considered which include: the geometry and the shape of the fins, air and water flow rates, and the heat exchanger size. In addition, the economic and environmental issues in the industry place the need for system compactness and further performance improvement. These requirements lead to the improvement of thermal performance, minimization of pressure drop, and easy fabrication.

Genhart (1962) designed a MICHX to boost the heat transfer rate from liquid to gas. Modern manufacturing industries are capable of making narrow channels heat exchangers due to the advancement in materials and methodology for a wide range of applications, especially in the areas of HVAC-R condensers, evaporators, automotive, and aerospace. The heat transfer process in minichannel heat exchangers depends on the heat transfer surface area (A_s), which is proportional to the channel hydraulic diameter (D_h). The liquid flow rate depends on the cross sectional area of the channel (A_c) which is proportional to Dh2. Thus, the ratio of the heat transfer surface area to volume (A_s/ v) corresponds to 1/D. As D decreases, the A_s / v increases (further compactness). On the other hand, Nusselt number for fully developed laminar flow is equal to Nu, an increase in h is obtained by decreasing D_h since, $_h$ is inversely proportional to the channel diameter. Therefore, by decreasing the heat exchanger channel diameter (D_{ch}), the heat transfer coefficient (h) will increase providing further compactness of the heat exchanger.

Motivations

MICHXs are used in different types of industrial applications with various geometries. Their enhanced heat transfer and small passage channels are the main characteristics that differentiate them from other heat exchangers. A multiport flat slab minichannel heat exchanger (MICHX) is becoming more prevalent among heat exchangers. This aluminum multiport slab MICHX is predicted to be a superior candidate over conventional heat exchangers for the following reasons:

- Higher thermal performance.
- Compactness: Its area density is nearly 4000 m^2/m^3, almost six times higher than the traditional compact heat exchangers, Carrier (2006) and Kim and Groll (2003).
- Diminished both air and water sides pressure drop for a given heat duty, Kang et al. (2002) and Fan (2008).
- Lower pressure drop reduces fan size, hence decreases the energy consumption for driving the fan and its noise (environmentally friendly).
- More structural robustness since the slab structure is monolithic and more reliable compared to the tube row with the connection joints.
- It prevents structural failure due to its resistance to the vortex induced vibration and is environmentally friendly (sound pollution). Therefore, it is recommended for the HVAC-R applications, Carrier (2006).
- The serpentine effect leads to the axial heat conduction phenomenon which in turns causes a secondary flow and develops new boundary layer that result in an increase in the heat transfer rate, Dehghandokht et al. (2011).

Objectives

The objective of the present study is to investigate the heat transfer characteristics of heating the air-side and cooling the liquid-side of a serpentine slab minichannel heat exchanger. The investigation determines the effect of the serpentine bend, the presence of the axial heat conduction, and viscous dissipation in the MICHX. The heat transfer correlation found from this current study is compared to the other available correlations. The following are the key objectives of this investigation.

- Experimentally analyze the heat transfer characteristics (h, Nu) of the airside heating and DI water cooling in a minichannel heat exchanger.
- Examine the prototype heat exchanger performance, overall thermal conductance (UA), heat exchanger effectiveness ( ), and the number of transfer units (NTU)
- Obtain the general correlations of both air and water side heat transfer and fluid flow such as Nu, h, NTU with Re, Nu with Br, and Nu with De.
- Compare the established correlations Nua-Rea-Pra of air heating with the correlations of air cooling obtained by Dasgupta (2011).
- Possible scope of improvements in the multiport prototype MICHX.

High flux heat removal with light weight and low area density is a roadmap of challenges and opportunities. Watchful achievements of such investigation objectives provide a source of information for forthcoming research.

II. REVIEW OF LITERATURE

The heat exchanger design is a field of thermal engineering that involves the conversion or exchange of thermal energy and heat between two or more fluids by various mechanisms such as by; conduction, convection, radiation and phase change. In recent years, considerable research and several investigations were applied to optimize the design of compact heat exchangers with

narrow channels. However, the literatures studying the air side characteristics using a minichannel heat exchanger with circular channels are rare. The Nu number found for minichannel heat exchangers is 0.21 to 16 times higher than that for conventional heat exchangers. Kandlikar and Shah (2006) classification is based on the channel size, which is widely used nowadays, is outlined in Table 1.1.

Table 1.1 Channel classifications, Kandlikar and Shah (2006)

Conventional passages	> 3 mm
Minichannels	3 mm ≥ D ≥ 200 μm
Microchannels	200 μm ≥D ≥10 μm
Transitional Microchannels	10 μm ≥ D ≥ 1μm
Transitional Nanochannels	1μm ≥D ≥ 0.1μm
Nanochannels	0.1μm ≥ D

Scaling Effect

The scaling effect describes the scale invariance found in many natural phenomena. Considering the scaling effect, some correlations used in conventional heat exchangers can be applied to minichannel heat exchangers working in the laminar regime. On the other hand, the applicability of other heat transfer characteristics is still under debate.

Tuckerman and Pease (1981) initially investigated the use of microchannels in a heat sink to cool the silicon integrated circuits. Inspired by Tuckerman and Pease's work, Morini (2004) investigated several experiments on single phase convective heat transfer in microchannels. Although a literature exists that covers the correlation used for a developing laminar flow in conventional pipes, the correlations concerned with the developing laminar flow in circular serpentine multi-slab MICHX are rare. Khan et al.

(2010) established a correlation for a single slab mini channel heat exchanger using 50% ethylene glycol-water mixture as the working fluid. The correlation found for that study was **$1400 \geq Re_a \geq 400$**, for Reynolds number range of $Nu = 0.152\, Re_g^{0.4912} Pr_g^{0.33}$, which is higher than that for a fully developed flow in conventional heat exchangers. Dasgupta (2011) studied the air side of a mini channel heat exchanger using DI-water as the working fluid. The correlation was found from his study is $1400 \geq Re_a \geq 400$, $Nu_a = 0.3972\, Re_a^{0.3766}$, he noticed that Nu is higher than Tang and Tailor's (2005). The main advantages minichannel heat exchangers provide over conventional compact heat exchangers considering the same heat transfer duty are: smaller size, lighter weight, larger heat transfer area density (m^2/m^3), lower fluid waste and less pollution for some fluids like Freon, higher heat transfer coefficient and energy efficiency.

Axial Heat Conduction In The Channel Wall

Gamrat et al. (2005) numerically analyzed the entrance and conduction effects in rectangular micro channel heat sinks. Two and three dimensional numerical models with 1mm and 0.1 mm channel spacing were studied. In their study, water was used as the working fluid with Reynolds number range of 200 to 3000. The numerical simulation results found to have a good agreement with the published data on flow and heat transfer in two dimensional channels. Results show that the entrance effect is dependent on Reynolds number and the channel spacing, which are not the same found for the reference case of uniform inlet velocity and temperature profiles reported by Shah and London (1978). The numerical models used in their work assumed some simplifications, e.g. viscous heating was not taking into account, which can decrease the Nusselt number especially for channels of smaller spacing than those investigated in the current work. There was no size effect on heat transfer showed when the channel spacing is reduced from 1mm down to 0.1 mm. As a result, the strong reduction in Nusselt number observed in the experiments cannot be explained due to conduction effects such as the axial conduction in the walls or deficient of two-dimensionality of the heat flux distribution since the geometry is complex.

Zhuo et al. (2007) experimentally and numerically investigated 3 different rough tubes and 3 other different soft tubes with Dh =50 1570 and de-ionized water to cool the water at Re= 20 ˜ 2400. Axial heat conduction (AHC) was studied numerically. The effect of AHC weakened as Re increased and relative tube wall thickness decreased, thus the local Nu approached the conventional theory prediction. Axial heat conduction number M is a dimensionless number that was used to express the relative importance of the axial heat conduction in the tube wall over the convective heat transfer of the fluid flow in the tube. M is not the only criterion for judging whether the axial heat conduction can be neglected. When increasing Re to more than 100, the results agreed with the traditional heat transfer characteristics.

$$M = \frac{\emptyset_{cond}}{\emptyset_{conv}} = \frac{A_{c,o} K_s \Delta T_s / L_h}{A_{c,i} \rho C_p u_{ave} \Delta T_l} \quad (2\text{-}1)$$

Where

$$A_{c,i} = \pi R_i^2, \text{ and } A_{c,o} = \pi (R_o^2 - R_i^2)$$

$$\Delta T_l = T_{b,avg} - T_{in} \quad (2\text{-}3)$$

$$\Delta T_s = T_{s,out} - T_{in}$$

The heat conduction of water in mini-micro channels was numerically investigated by Maranzana et al. (2004). The wall heat flux density, for small Reynolds numbers, can become strongly non-uniform: most of the flux is transferred to the fluid flow at the entrance of the mini–micro-channel. Another finding was that axial heat conduction in the walls of a mini–micro counter-flow heat exchanger yielded a loss of efficiency: an optimal wall conductivity that maximized this efficiency existed. A new non-dimensional number, axial conduction number (M) quantifying the relative part of conductive axial heat transfer in walls has been introduced. Disregarding this effect can lead to very large bias in the experimental estimation of heat transfer coefficients, especially for small Reynolds numbers. Even if the non-dimensional numbers (Br_w, and NTU) and boundary conditions have an effect on axial conduction too, it has been noticed that in the simulation of most cases that were studied, axial conduction can be neglected as soon as the M number becomes smaller than 10^{-2}. Axial conduction in the walls has to be considered for the design of mini channel heat exchangers. There existed an optimal conductivity for the wall which maximized the exchanger efficiency.
Cole and Cetin (2011) numerically studied axial conduction both in the fluid and in the adjacent wall for heating using a parallel-plate microchannel. A uniform heat flux was applied to the outside of the channel wall. The fluid was liquid with constant properties and a fully-developed velocity distribution. The study included obtaining numerical results for the local and average Nusselt number for various flow velocities, heating lengths, wall thicknesses, and wall conductivities. These results have applications in the optimal design of small-scale heat transfer devices in areas such as biomedical devices, electronic cooling, and advanced fuel cells. It was found that the effect of the axial conduction in the channel wall is important when: (i) the microchannel has a small length-over-height ratio; (ii) the Peclet number (Pe) is small; (iii) the wall thickness relative to the channel height is large; and, (iv) the wall conductivity of the wall material is high relative to the thermal conductivity of the working fluid. For high Pe flow (e.g. Pe> 100) along with a low thermal conductivity wall, the effect of the axial conduction in the wall is negligible.

The Minichannel Heat Exchanger (MICHX)

Forced convection heat transfer in a cross-flow microchannel heat exchanger was experimentally investigated by Cao et al. (2010). The maximum volumetric heat transfer coefficient found with DI-water as the working fluid reached 11.1MW.m-3.K-1 with a corresponding pressure drop of less than 6 kPa when Reynolds number in the microchannels was ~64. Furthermore, the maximum volumetric heat-transfer coefficient using air as the working fluid was 0.67 MW.m-3.K-1 at a corresponding pressure drop of ~30 kPa when Re ≈ 1026. Correlations of the average Nusselt number and Re values were obtained from the main cryogenic heat exchanger (MCHE) with 2 plates and their validity was confirmed by other MCHEs with 2 and 10 plates.

III. DESIGN AND METHODOLOGY

Key Assumptions

The following assumptions were made to facilitate data reduction and proper evaluation.

- Experiments were conducted at steady state.
- Heat transfer due to radiation is negligible.
- No heat loss from the test chamber to the surrounding.
- No condensation on the surface of the heat exchanger.

Heat Balance (HB)

It is assumed that the test chamber is well insulated and there is no heat loss between the test chamber and the surrounding. In other words, the heat transfer from the airside and the liquid side should be considered equal. As this assumption is not valid for a practical case, it is necessary to estimate the heat balance based on the percentage of liquid-side heat transfer compared to the ideal case. In real applications, HB cannot be zero and its equation can be written as,

$$HB = \left(\frac{\dot{Q}_w - \dot{Q}_a}{\dot{Q}_w}\right) * 100 \quad (3\text{-}33)$$

For more accurate results, the HB can be calculated based on the average heat transfer rate instead of the liquid heat transfer rate and the equation is expressed as,

$$HB_{avg} = \left(\frac{\dot{Q}_w - \dot{Q}_a}{\dot{Q}_{avg}}\right) * 100 \quad (3\text{-}34)$$

The average heat transfer rate is found as,

$$\dot{Q}_{avg} = \frac{\dot{Q}_a + \dot{Q}_w}{2} \quad (3\text{-}35)$$

It is worthy to note that the ASME PTC 30-1991 acceptance of the heat balance HB range is limited to ± 15%.

Heat Transfer Performance

Overall Thermal Conductance (UA)

The thermal resistance is a material property and a measure of the resistance of the material to the heat flow. The total thermal resistance can be calculated as,

$$R_{total} = R_a + R_{wall} + R_w \quad (3\text{-}38)$$

Where are the thermal resistances of air, wall and water, respectively. The notation is the fin effective ess or the fin airside extended surface efficiency. It is calculated as,

$$R_a = \frac{1}{(\eta hA)_a}, R_{wall} = \frac{\ln\left(\frac{d_o}{d_i}\right)}{2\pi k_{al} L}, R_w = \frac{1}{(hA)_w}, -\eta_f) \quad (3\text{-}39)$$

Where, n_f is the fin efficiency and it depends on the fin geometry and arrangement. is the fin area and is the total heat transfer surface area of the airside. Accordingly, the overall thermal resistance can be estimated as,

$$UA = \frac{\dot{Q}_{avg}}{F\Delta T_{LMTD}} \quad (3\text{-}40)$$

Where, UA is the overall heat coefficient based on the surface area and F is the log mean temperature difference correction factor for a cross flow heat exchanger. In this study, F has been considered as a unity.

Effectiveness (ε̇)

The heat exchanger performance is usually characterized by its effectiveness (ε̇) and number of transfer units (NTU). Effectiveness can be calculated as,

$$\varepsilon = \frac{\dot{q}}{\dot{q}_{max}} = \frac{\dot{q}}{(\dot{m}c_p)_{min}\Delta T_{max}} \quad (3\text{-}41)$$

In the current investigation, the minimum heat capacity rate was found on the waterside and the maximum temperature difference is between water inlet (Tw,i) and air inlet (Ta,i). Rearranging the above equation, can be rewritten as;

$$\varepsilon = \frac{\dot{q}}{(\dot{m}c_p)_w (T_{w,i} - T_{a,i})} \quad (3\text{-}42)$$

Number of Transfer Units (NTU)

The number of transfer units (NTU) is defined as the ratio of the overall thermal conductance (*UA*) to the minimum heat capacity rate C_{min} as,

$$NTU = \frac{UA}{C_{min}} = \frac{UA}{(\dot{m}C_p)_w} \quad (3\text{-}43)$$

It is considered a design parameter for heat exchangers and it is an indication of the non dimensional thermal size rather than the physical size of exchangers.

Pressure Drop

The pressure drop is considered a vital factor that plays an important role in the heat exchanger performance. The total pressure drop through the heat exchanger core depends on the geometric parameters, the fluid types, and the thermodynamic properties. Hereafter, some important parameters such as the friction factor (f), entrance effect, and pressure drop in the straight tube and the curved tube are expressed.

$$f_d = \Delta P \frac{D}{L} \frac{2}{\rho V^2} \quad (3\text{-}44)$$

The friction factor is used to determine the pressure drop for fully developed or developing laminar flow as illustrated below,

$$\Delta P = \frac{f_d L \rho V^2}{2D} \quad (3\text{-}45)$$

Where, p is the channel circumference. The Hagen Poiseuille theory expresses the pressure drop in a fluid flowing through a long cylindrical pipe. It is mentioned that after a fluid enters a channel or a tube, the velocity profile begins to develop through the channel until it is fully developed. The velocity is assumed to be uniform at the entrance and the pressure drop in the minichannels is substantial. Hence, the pressure drop caused by the entrance effect should be taken into consideration. If the entrance length is very small in comparison to the total length, the entrance effect may be ignored.

Pressure Drop in the Straight Tube:

There are two significant lengths in the tubes: the hydrodynamic entrance length and the thermal entrance length. The entrance lengths indicate the flow character. For a laminar flow, the hydro dynamically developing length is proportional to Re and can be found through the following equation,

$$L_{hy} = 0.05 Re D_h \quad (3\text{-}46)$$

The thermal entrance length can be estimated as,

$$L_{th} = 0.05RePrD_h \quad (3\text{-}47)$$

Or

$$L_{th} = 0.05\frac{\rho V c_p D_h^2}{k} \quad (3\text{-}48)$$

For fully developed flow, the pressure drop is found as,

$$\Delta P = \frac{128\mu LAV}{\pi D^4} \quad (3\text{-}49)$$

$$\Delta P = \frac{L}{D}\frac{32\mu V}{D} \quad (3\text{-}50)$$

Where, D is the channel diameter, L is the flow length, V is the flow velocity, and μ is the dynamic viscosity.

IV. EXPERIMENTAL SETUP

The current experiments were conducted through a well-designed and instrumented experimental setup as shown in Fig. 4.1. It consists of a closed-loop integrated thermal wind tunnel, test chamber, liquid circuit with heater, various measuring and monitoring instruments, a built-in heat exchanger that maintains the inlet-air temperature, wavyfinned serpentine cross-flow minichannel heat exchanger, variable speed gear pump that provides the flow of the fluid, and a 16 bit LabView data acquisition system that monitors and records all data. The largest component of the setup is the integrated closed-loop thermal wind tunnel.

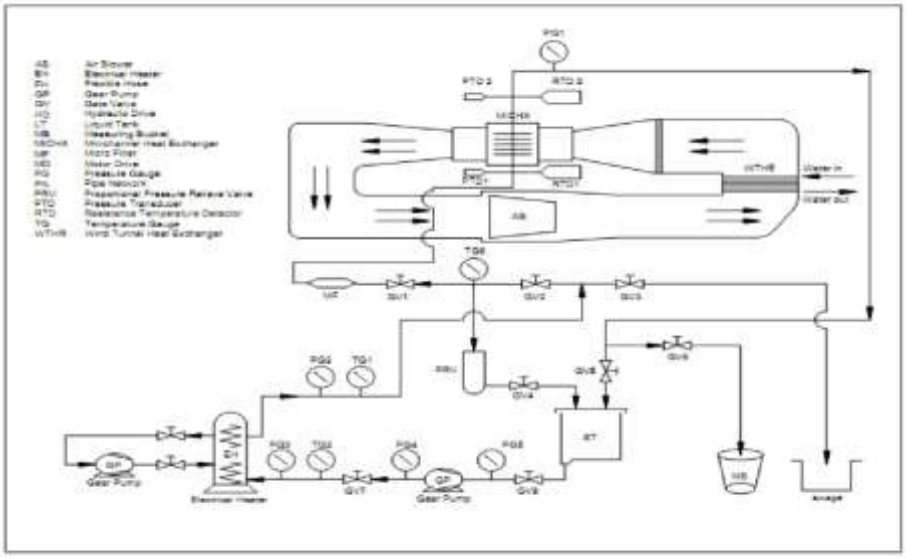

Figure 4.1 Schematic diagram of the experimental setup

Calibration

A calibration procedure should be applied at the same experimental conditions. Preceding any experiment, the inlet and outlet RTDs, PTDs, and thermocouples on both air and DIwater sides were calibrated using the thermocouple and RTD calibrators. These experiment results were recorded and entered into the National Instrument data acquisition system.

Data Acquisition System (DAQ)

The data acquisition system (DAQ) is the main and highly accurate part of the system that records all the data needed to perform the analysis. The main components of the DAQ system are:

Data Acquisition System Software (LabView)

The Laboratory Virtual Instrumentation Engineering Workbench (LabView version 8), which is produced by National Instruments, is used in the current system. It collects all the data at a sampling rate of 100 kHz. It is supported by a National Instrument data acquisition card, NI-PCI-6052E multi-function I/O Board that is connected to the PC.

SCXI Signal Conditioning

The devices in the DAQ system that collect electrical signals from the measuring devices are called signal conditioning. An SCXI signal conditioning consists of multichannel signal conditioning modules placed in one or more rugged chassis. The signals come from thermocouples (TCs), RTDs, PTDs, and flow meters and are processed by the LabView software to present the final data.

Terminal Block Model SCXI-1300/1303

The terminal block has 32 available channels and is connected to the modules through screws which in turn are connected to the chassis. The terminal block can conveniently connect input signals such as RTDs, PTDs, thermocouples, and flow meters.

Figure 4.16 Terminal Block model SCXI -1300/1303

Module SCXI-1102

The Module SCXI- 1102 sets signals as legible by the 16-bit data acquisition card (NI 6052E). More than 300 analog signals are collected from RTDs, PTDs, and TCs from different voltage and current sources that are required to process the data.

SCXI-1000

The SCXI-1000 is a chassis that holds the terminal block as well as the modules and supply the power to them.

Data Acquisition Card

The data acquisition card is a switchless, jumperless data acquisition (DAQ) card. It is connected to the PC and transfers the data from the DAQ to the PC. The system has 128 channels for acquiring data. It is able to monitor, read, and record 96 individual parameters through 96 channels at a rate of 100 Hz.

Flow Kinetics (FKT)

The Flow Kinetics device used in the experimental set up measures the pressure, relative humidity, density, and the temperature of the air side. The make and model of the device is Flow Kinetics TM-LLC /FKT-3DP1A-0.4-5-1. Pressure measurements include: an absolute pressure (Pabs) and three differential pressures (P1, P2, P3) concurrently for the airside inside the wind tunnel. The sample rate in the present study is 1 kHz for accuracy and consistency.

Minichannel Heat Exchanger MICHX

The serpentine slab minichannel heat exchanger is constructed of 15 multiport aluminum serpentine slabs in three circles as illustrated in Figures 4.18 and 4.19. Each slab is 2 mm thick and has 68 circular channels with inner hydraulic diameters of 1 mm. The frontal area of the MICHX is 304mm X 304 mm. The MICHX is capable of sustaining 15 MPa working pressure. The de-ionized water (DI water) coming from the inlet header is distributed into three inlet manifolds and passed through the three circuits. After participating in the heat transfer, it leaves the heat exchanger core through three outlet manifolds and an outlet header.

Figure 4.18 Minichannel heat exchanger, front and side view

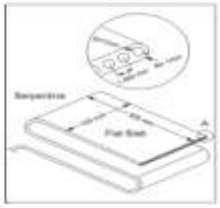

Figure 4.19 Minichannel serpentine flat slabs

Table 4.2 Specifications on the liquid side of the MICHX

Hydraulic diameter	0.01 m
Minichannel slab height	0.02 m
Number of header(inlet &outlet)	2
Number of flow passes	3
Number of slabs in a circuit	5
Total number of slabs	15
Number of channels per slab	68
Total heat transfer area-waterside	974.7×10^{-3} m^2

The specifications of the liquid side of the MICHX are given in Table 4.2.

Experimental Methods and Operating Conditions

In this study, the thermal performance and flow behavior of the working fluid, Di-ionized water and air, in a prototype multiport mini-channel heat exchanger were investigated for air heating. The DI-water was passed through the prototype multiport minichannel heat exchanger at a constant temperature of $70^{\circ}C \pm 0.5^{\circ}C$. Three essential variables including DI-water mass flow rate (T_w), air inlet temperature (T_a), and air velocity (V_a) are used to study the fluid flow and heat transfer behavior. Mass flow rate was changed from 1.35 kg/s to 2.15 kg/s that corresponded to Rew of 255 to 465. Air inlet temperature varied from $25^{\circ}C \pm 0.5^{\circ}C$ to $38^{\circ}C \pm 0.5^{\circ}C$ at 5 steps ($26^{\circ}C$, $29^{\circ}C$, $32^{\circ}C$, $35^{\circ}C$, $38^{\circ}C$). The air velocity passing through the heat exchanger core diverted from 6m/s to 18 m/s at 4 steps (6m/s ,10,m/s 14m/s,18m/s) that corresponded to Rea of 1650 to 5317 for each DI-water mass flow rate.

Table 4.3 The operating conditions

Inlet DI-water temperature °C	Inlet air temperature °C	Air Velocity m/s	DI-Water mass flow rate Kg/s
70	26	6, 10, 14, 18	0.022, 0.029, 0.035
70	29	6, 10, 14, 18	0.022, 0.029, 0.035
70	32	6, 10, 14, 18	0.022, 0.029, 0.035
70	35	6, 10, 14, 18	0.022, 0.029, 0.035
70	38	6, 10, 14, 18	0.022, 0.029, 0.035

V. ANALYSIS OF RESULTS

DE-IONISED WATER PROPERTIES

Density

De-ionised water is just what it sounds like, water that has the ions removed. The reason that in this experiment deionised water is used is that ions cause interference while an experiment is running. They can switch place with other ions. Water with ions in it is also quite a lot more electrically conductive than water without ions.

The variation in density of DI-water with temperature is shown in Figure 5.1. The change in the water density is less than 2 percent for the temperature range of the case study Ma (2007). There is not much changes in other properties of DI-water such as specific heat, dynamic viscosity , and conductivity k.

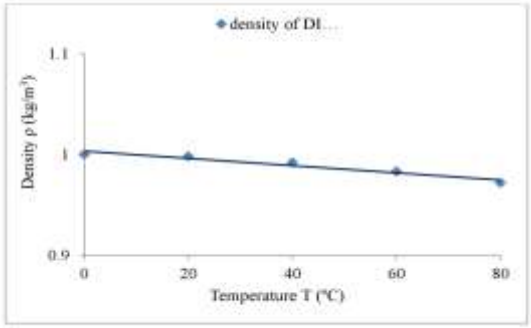

Figure 5.1 The effect of temperature on the density of water

Deionised Water Properties

System Heat Balance (HB)

According to ASME PTC-1991, it is set that all the data collected in the defined operating condition is accepted in the range of ±15%. As shown in Figure 5.2, our current experimental data is between which indicates that the heat loss to the surroundings is negligible due to proper heat insulation of the test section. The validation of these data confirms its suitability to be used for heat transfer calculations.

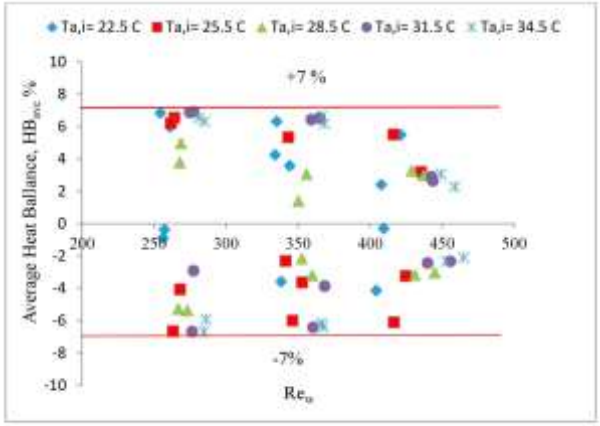

Figure 5.2 Heat balance vs. water Reynolds number

Effects of R_{ew} on $T_{a,i}$ and $T_{a,o}$ of DI-Water

The effect of Rew on the water temperature drop (T_w) in the heat exchanger is illustrated in Figure 5.3. The inlet-outlet temperature differences are higher at lower Re and lower at higher Re. Thus by increasing the R_{ew}, the T_w will decrease. The

trend shows that for a specific high R_{ew} the temperature drop will be insignificant. It is also shown that the R_{ea} has a minimum influence on the temperature drop.

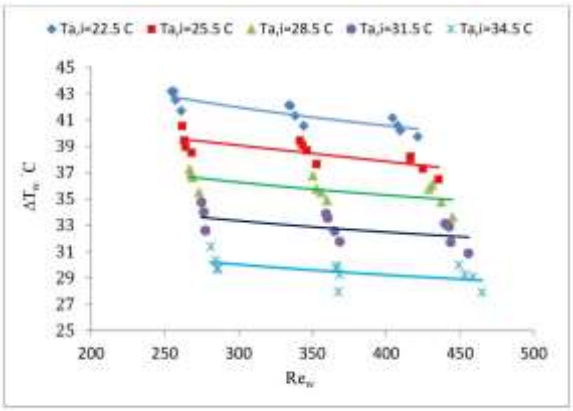

Figure 5.3 Effects of water side Reynolds number on the temperature drop

Effect of R_{ew} on Normalized Heat Transfer

The normalized heat transfer (Q*) has an immense role in analysing the heat transfer characteristics. It is defined as

$$Q^* = \frac{\dot{Q}}{A_F(T_{w,i} - T_{a,i})} \qquad (5\text{-}1)$$

Where, Q* is the normalized heat transfer rate, Af is the frontal area of the heat exchanger, T_{wi} and T_{ai} are the water and air inlet temperatures, respectively. The effect of Rew on Q* is plotted in Figure 5.4 It is revealed that Q* is dependent on R_{ew} and increases with the increase of Rew. The following correlation demonstrates a power law relation.

$$Q^* = 0.012\, Re_w^{0.894} \qquad (5\text{-}2)$$

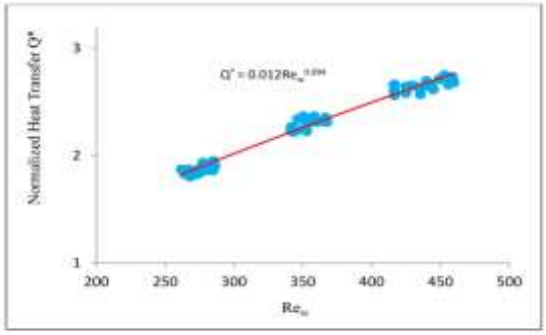

Figure 5.4 The effect of water-side Reynolds number on normalized heat transfer (Q^*)

Effect of Rea on Air and water heat transfer rate

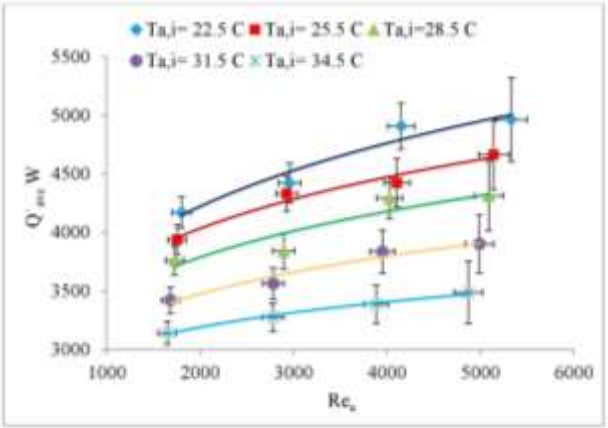

Figure 5.5 The effect of Re_a on the average heat transfer rate

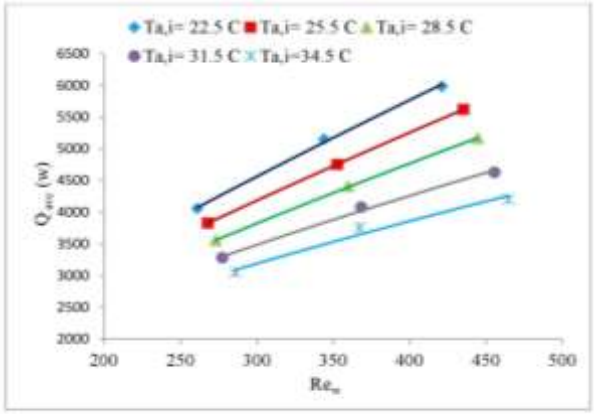

Figure 5.6 The effect of Re_a on the average heat transfer rate

Effect of Rea on LMTD

Log Mean Temperature Difference (LMTD) is used to determine the temperature motivating force for heat transfer in flow systems, most remarkably in heat exchangers. The size and the heat transfer area could be found using LMTD method. LMTD is

a normalized parameter that can be used to compare two different heat exchangers. The large the LMTD, the more heat is transferred. Figure 5.7 shows the effect of Rew on LMTD for different temperatures of water. The power law was the best curve fit. It is found from the figure that the highest LMTD belongs to the lowest $T_{a,i}$ for a constant R_{ew}. The illustration also shows that the LMTD is elevated as R_{ew} is enlarged.

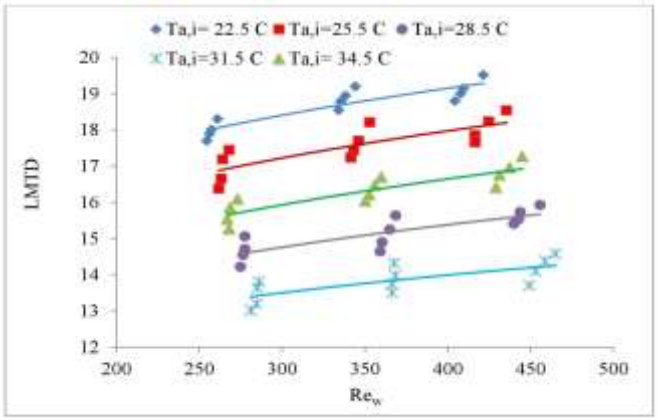

Figure 5.7 The effect of Re_w on LMTD

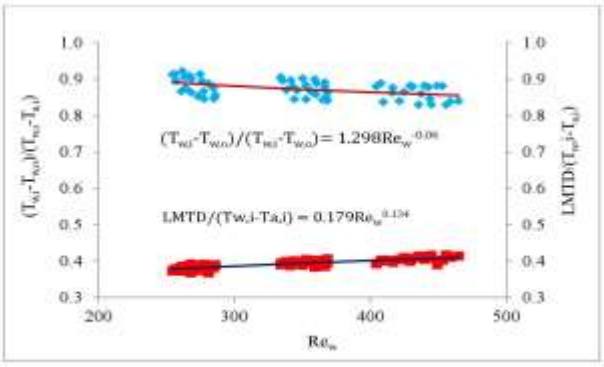

Figure 5.8 The effect of Re_w on $T_{non\text{-}dimensional}$

Effect of Rew on LMTD

There are two dimensionless temperature quantities used in heat exchangers which are named as LMTD-dimensionless and ΔT - dimensionless. The dimensionless ΔT is expressed in Equation (5-3) as the ratio of the temperature change in the water side to the maximum temperature difference between the two fluids in heat exchangers.

$$\Delta T_{dimentionless} = \frac{T_{w,i} - T_{w,o}}{T_{w,i} - T_{a,i}} \qquad (5\text{-}3)$$

The LMTD-dimensionless is described in equation (5-4) as the ratio of LMTD to the maximum temperature difference, water and air inlet temperatures.

$$LMTD_{dimentionless} = \frac{LMTD}{T_{w,i} - T_{a,i}} \qquad (5\text{-}4)$$

Figure 5.8 illustrates the relation between R_{ew}, LMTD-dimensionless, and ΔT dimensionless. It demonstrates that by increasing R_{ew}, LMTD-dimensionless will be reduced, and on the contrary the $\Delta T_{dimensionless}$ will be increased as expected. The plot includes all the air temperatures and velocities. The slope of both curves flattens as R_{ew} increases.

Effect of R_{ew} on N_{uw}

The water side and air side Nusselt number (Nu_w) verses Rew for the 5 different air temperatures and velocities are illustrated in Figure 5.9. The correlation is a power law curve-fit with a positive exponent. The slope of the trend is gentler as Re increases. A correlation established for Nu_w on R_{ew} is given below,

$$Nu_w = 1.87\ Re_w^{0.15} \qquad (5\text{-}5)$$

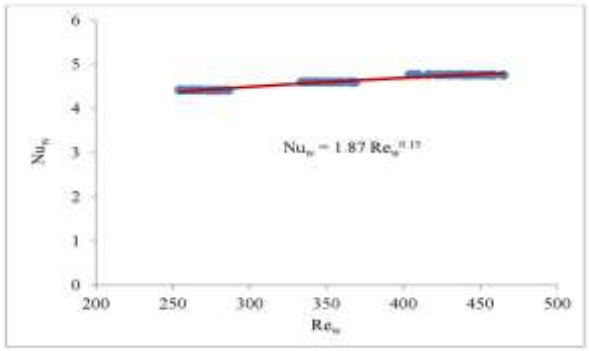

Figure 5.9 The effect of Re_w on Nu_w

Effect of R_{ew} on Nuw, and P_{rw}

The relationship between the non-dimensional parameters; water-side Reynolds number, and Prandtl number on water-side Nusselt number, has been investigated. The effect of R_{ew}, P_{rw} on Nu_w is plotted in Figure 5.10. The investigation shows that Nuw will increase with the increase of R_{ew} and P_{rw}. The dependency of Nu on Re, and Pr followed the power law relation. The water-side heat transfer general correlation is obtained in the form of Nusselt number as a function of water-side Reynolds number and Prandtl number shown as,

$$Nu_w = 1.2\ Re_w^{0.17}\ Pr_w^{0.33} \qquad (5\text{-}6)$$

Khan et al. (2010) performed an investigation on ethylene glycol-water mixture for a similar MICHX to characterize the heat transfer and fluid flow behaviour. They found a correlation of Nug=0.152 Pr0.33 for the developing fluid. The current results Nuw compare reasonably well with their findings. The differences between the results are due to the difference in liquid properties of DI- water and ethylene glycol-water, number of slabs which was 2, whereas for this study it is 15 slabs in three circuits, and also the range of Reynolds number of water which was 400-1900 compared to the current study of 257 to 411.
The Nusselt number should be 3.66 for the laminar developed flow in circular shape geometry under constant surface temperature boundary condition. In this investigation, Nu_w was calculated to be between 4.41 and 4.76 at constant property condition. This discrepancy is attributed to the developing flow regime in channels and the deviation from the ideal case of constant surface temperature.

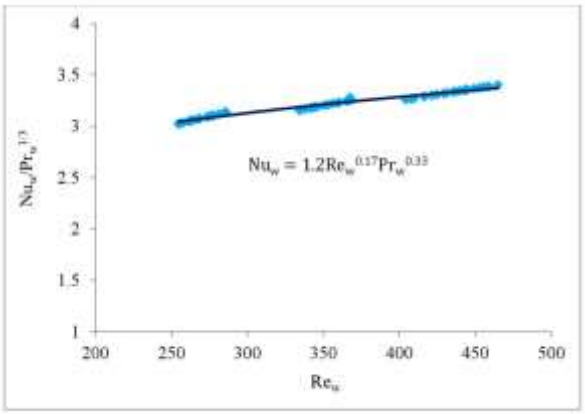

Figure 5.10 The effect of Re_w and Pr_w on Nu_w

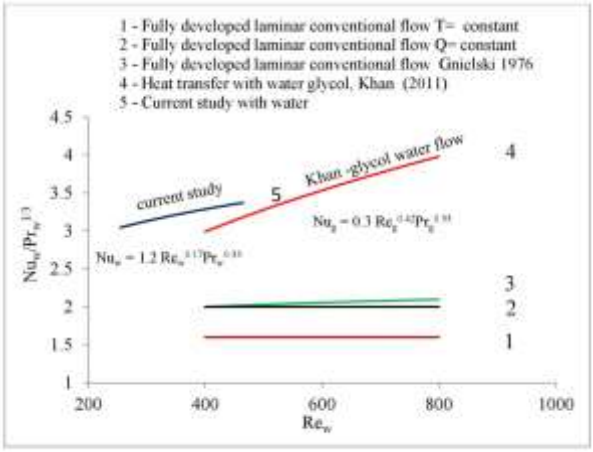

Figure 5.11 A comparison of the current correlation (Re_a, Nu_a, Pr_a)

Effect of Re_a on Nu_a, and Pr_a

The effect of Re_a and Pr_a on Nu_a has been investigated and the result is demonstrated in Figure 5.12. The best curve fit practiced as power law relation. As Re_a and Pr_a increase, Nu_a will increase. Since air is not a high viscous fluid, therefore its Prandtl number, which is a function of viscosity and conductivity, doesn't have a lot of variation and can be considered as a constant. At the bulk temperature, the correlation is found as,

$$Nu_a = 0.315\ Re_a^{0.373}\ Pr_a^{0.33},\ \text{for } 1750 > Re_a > 5750,\ 0.71 > Pr_a > 0.72 \qquad (5\text{-}7)$$

or

$$Nu_a = 0.281\ Re_a^{0.373},\ \text{for } 1750 > Re_a > 5750,\ 0.71 > Pr_a > 0.72 \qquad (5\text{-}8)$$

The Nu_a-Re_a-Pr_a correlation in equation (5-7) for the current study is compared to the correlation developed by Dasgupta (2011) for air cooling using the same MICHX in a Reynolds number range of 283 < Re_a <1384 as,

$$Nu_a = 0.529\ Re_a^{0.275}\ Pr_a^{0.33},\ \text{for } 283 > Rea > 1384,\ 0.71 > Pr_a > 0.72 \qquad (5\text{-}9)$$

Figure 5.12 shows that the heat transfer performance of the current study for the air heating followed the trend of air cooling established by Dasgupta (2011) with a slightly higher value for the heating mode.

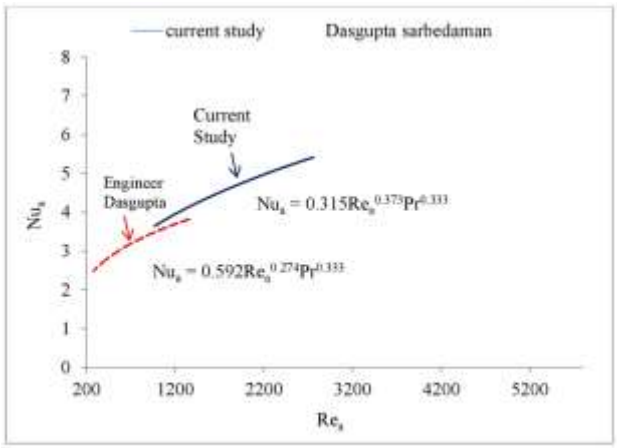

Figure 5.12 A comparison of the current correlation (Re_a, Nu_a, Pr_a)

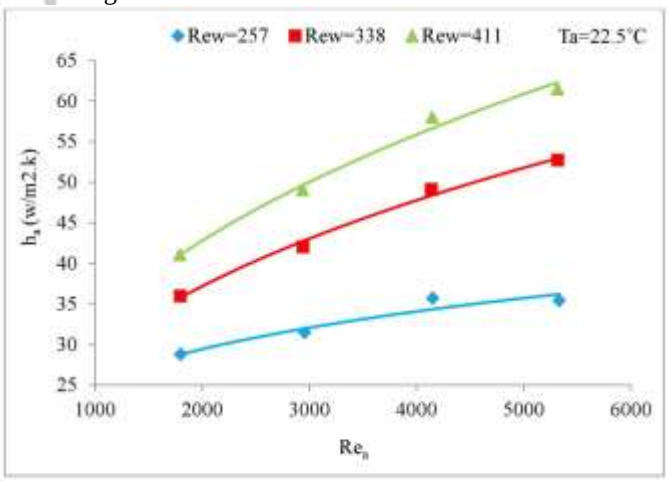

Figure 5.13 The effect of Re_a on h_a

Air-side heat transfer coefficient (h_a)

Air side heat transfer coefficient (h_a) can be calculated by an iteration method. Figure 5.13 shows the effect of Re_a on ha, while keeping the water side Reynolds number Re_w constant. It is obvious from the curve that h_a increases with the increase in Re_a, however the effect of Re_a on h_a is less compared to the effect of Re_w on ha. An instant change of Re_a from 1800 to 5300 affects h_a to change from 29.6 to 40.7, while varying Re_w from 257 to 411 for a constant Re_a=5300, h_a varies from 40.7 to 59.5. Thus convection heat transfer in mini-channel heat exchangers, Re_w has a dominating role in heat transfer occurrences.

Air-side Nusselt number (Nu_a)

The effect of the Rea on Nu_a is plotted in Figure 5.14 for constant air inlet temperature and different Re_w. The air-side Nusselt number is varied from 4.3 to 6.3 while Rea changes from 1800 to 5300. The variation of Re_w from 257 to 411 changes Nu_a from 6.3 to 7.6. This effect difference of Re_a and Re_w on Nu_a is similar to the effect on h_a. Therefore, the velocity of air has very smaller effect on Nu_a than Re_w.

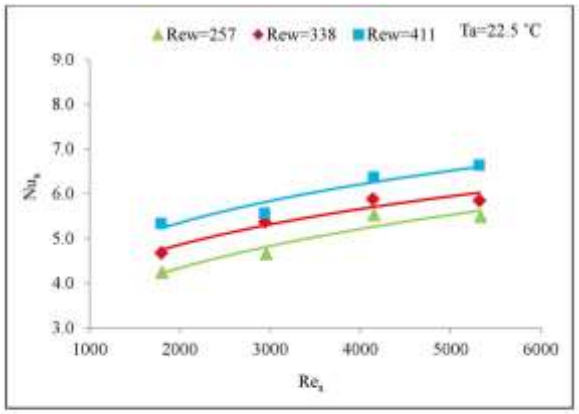

Figure 5.14 The effect of the Re_a on the Nu_a

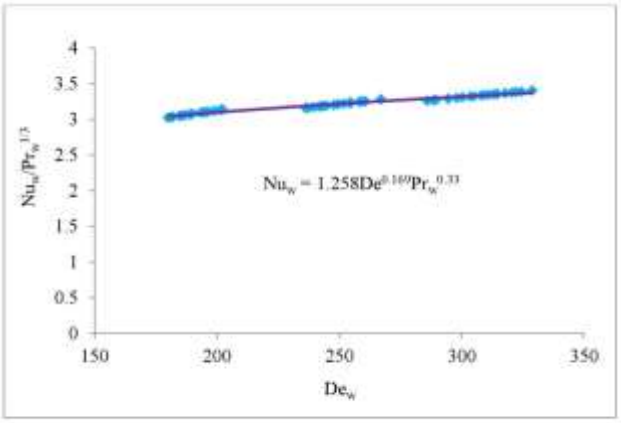

Figure 5.15 The effect of water-side Dean number on $Nu_w/Pr_w^{1/3}$

Serpentine Effect

The Dean number is a dimensionless number in fluid mechanics which takes place in the study of flow in curved pipes and channels. It represents the ratio of the viscous force acting on a fluid flowing in a curved pipe to the centrifugal force. In the current study the fluid passes through the serpentine path of the heat exchanger core which is a curved pipe. The study of Dean number is vital in analyzing the fluid flow behavior. De can be calculated from equation 3.16. Dean number of higher than 11.6, indicate that the curvature has a significant effect on the fluid flow characteristics. In the current study, Dean number was found to be from 182 to 315 which means that the friction factor in the straight part of the channel and the serpentine is different. In other words, the result shows that there is a secondary flow in the serpentine which disturbs the boundary layer in the curvature. At the exit of the bend, the boundary layer starts developing. This process intensifies the heat transfer rate. De is plotted against Nu_w and Pr_w in Figure 5.15.

The correlation for De established on Nu_w and Pr_w is shown as,

$$Nu_w = 1.258\ De^{0.17}\ Pr_w^{0.33} \qquad (5\text{-}10)$$

It predicts the serpentine effect on the enhancement of the heat transfer.

Viscous dissipation

Brinkman number, Br, is defined as the ratio of the heat production caused by the viscous forces to the heat transferred through the wall. It basically measures the viscous dissipation. Figure 5.16 presents the relation between the mass flux and Br. Brinkman number increases as mass flux increases by power law relation. It is calculated from equation (5.11). Br depends on the dynamic viscosity which is depends highly on temperature, so at low temperature the viscosity increases and more viscous dissipation occurs. Results from the study shows that Br lies between 5E-9 < Br < 1.334E-8. A practical correlation at a constant temperature boundary condition has been established as,

$$Br_w = 9E\text{-}14 G_w^{1.82} \qquad (5.11)$$

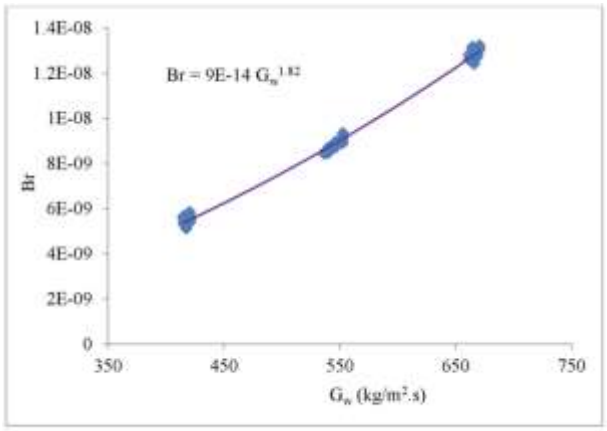

Figure 5.16 The effect of water-side mass flux on Brinkman number

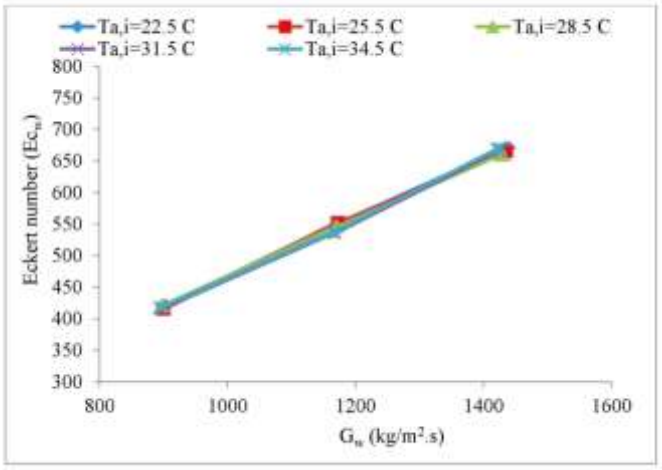

Figure 5.17 The effect of mass flux on Eckert number for the water side

5.5 Eckert number (E_c)

Eckert number is a non-dimensional number utilized in fluid dynamics. It states the relationship between kinetic energy and enthalpy of a flow and is employed to characterize dissipation through viscosity. The relation between Eckert, Brinkman, and Prandtl numbers is expressed as $Br_w = Ec_w.Pr_w$. E_c . Eckert number is plotted vs. mass flux (G_w) in Figure 5.17 and Nuw versus Ec in Figures 5.18 and 5.19. Ecw is calculated from the equation $E_c=V2/cp\ (Tb-T_{wall})$. The Br_w and E_c are both used to estimate the heat transfer characteristics and viscous dissipation. In the recent study, Eckert number was found within 1.6E-9 < Ec_w < 3.9E-9.

However, it is really small in scale but cannot be ignored owing to its influence on the viscous dissipation. Due to E_c being the ratio of kinetic energy of the fluid to the differential enthalpy at the boundary layer, it means that the kinetic energy is small compared to the enthalpy difference. While the kinetic energy increases with the increase of velocity or inertia, E_c increases which indicates that the viscous dissipation exists at a higher velocity and cannot be ignored. On the other hand, from E_c number equation, when T_{wall} increases, it results in an increase in T_b. The increase in T_{wall} leads to a decrease the viscosity, which in turns enhances the movement of the fluid molecules and results in a higher velocity, as well as an increase in E_c. The correlation established for the relation is found as,

$$Nu_w = 26.24\ Ec_w^{\ 0.088} \qquad (5\text{-}12)$$

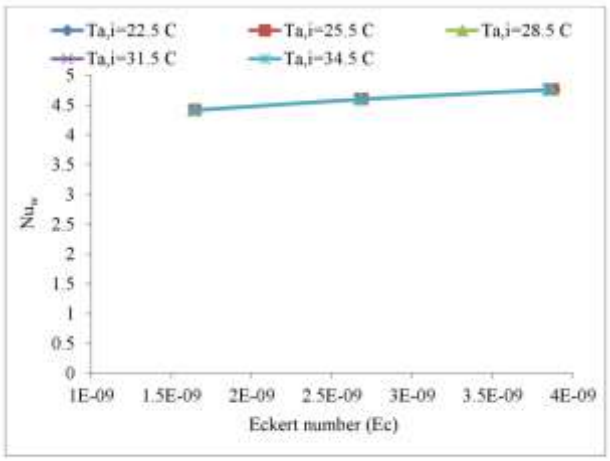

Figure 5.18 The effect of waterside Eckert number on Nu_w

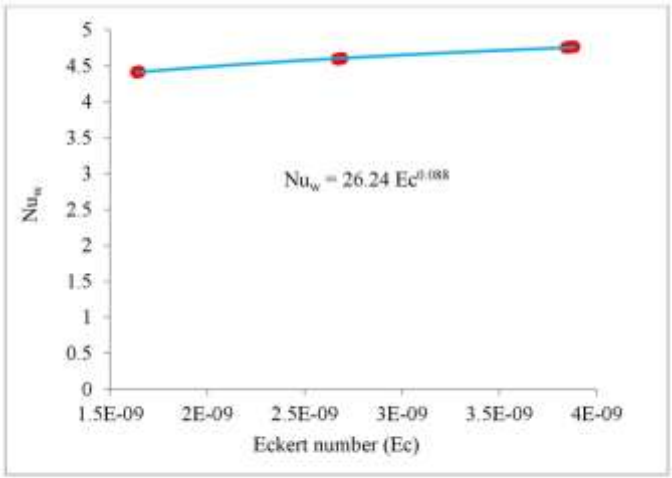

Figure 5.19 The effect of water-side Eckert number on Nu_w

Heat Exchanger Performance

There are two important factors in evaluating a heat exchanger performance; effectiveness (ε) and NTU.

Effectiveness (ε)

The effectiveness of the recent MICHX has been calculated from equation 3-42. Figure 5.20 demonstrates the effects of varying Re_a on effectiveness. It is revealed that ε increases by increasing Re_a in a power law curve. The slope of the curves from the figure indicates that the heat exchanger is at its

high effectiveness and the change of ε with Re_a is monotonous. It also shows that effectiveness is higher at a higher air inlet temperature. For the current study as Rea varies from 1750 to 5300 for a defined air inlet temperature between 22.5 C and 34.5 C, effectiveness change is found to be from 0.82% to 0.97%. Consequently the effect of Rea and Ta,i on effectiveness is diminutive.

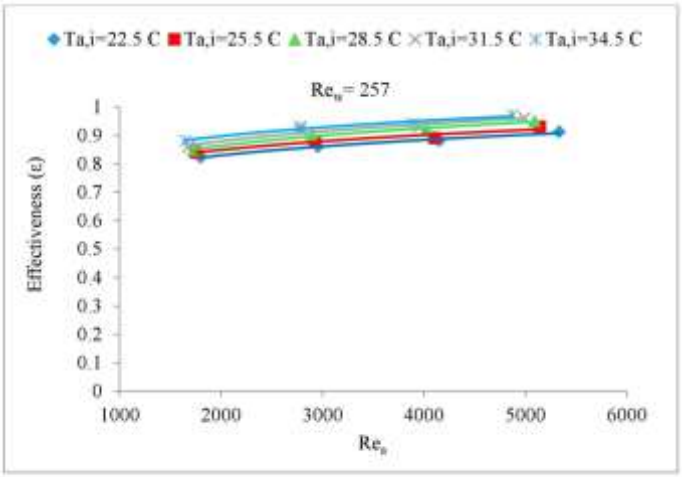

Figure 5.20 The effect of air-side Reynolds number on effectiveness

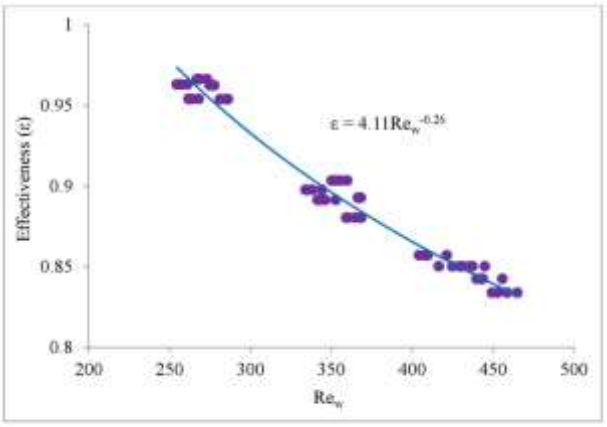

Figure 5.21 The effect of air-side Reynolds number on effectiveness

Figure 5.21 demonstrates the relation between ε and Re_w. Water Reynolds number was changed from 257 to 411. It is shown that ε increases with the increase in Re_w in a power law basis. Effectiveness is higher at lower Re_w. The reason is that at low Re_w, water flows at a low velocity, the dwelling time for water in the channels is higher which means more heat transfer and that leads to higher ε. The correlation found is,

$$\varepsilon = 4.11\ Re_w^{-0.26} \qquad (5\text{-}13)$$

As discussed previously, Re_w possess a higher effect than Rea and $T_{a,i}$. Thus, in optimizing a heat exchanger design, Re_w is considered as the more influential factor. These results agree with the study of Khan et al. (2010) using a similar heat exchanger but with two slabs where a similar correlation was obtained.

Number of Transfer Units (NTU)

The Number of Transfer Units (NTU) method is used to compute the rate of heat transfer in heat exchangers when there is a lack of information to determine the Log-Mean Temperature Difference (LMTD). In a heat exchanger analysis, if the fluid inlet and outlet temperatures are indicated or can be easily calculated from the energy balance equation, the LMTD method can be used. NTU is plotted against Rea in Figure 5.22. It is evaluated from equation (3-43). From the three figures, one can conclude that NTU increases by increasing Re_a and decreases when higher Re_w is used. It also clarified that Re_w has a dominant effect on NTU.

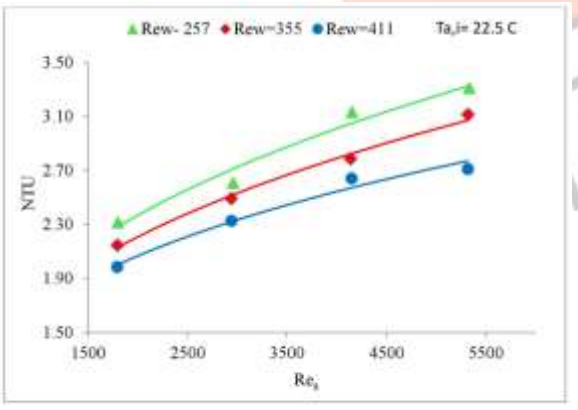

Figure 5.22 The effect of Re_a on NTU

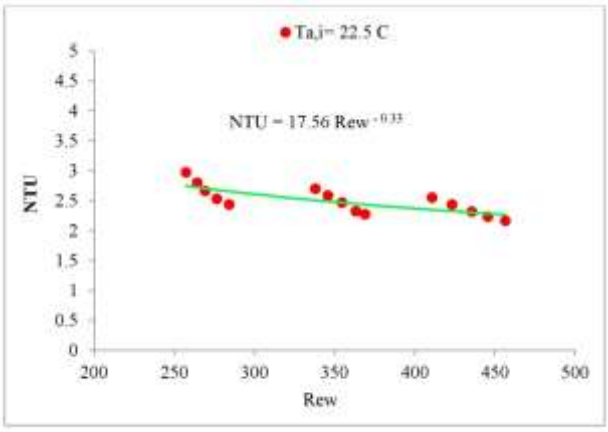

Figure 5.23 The effect of Re_a on NTU ($T_{a,i}$=22.5°C)

The effect of Re_w on NTU for 5 different air inlet temperatures is illustrated in Figure 5.23 and Figure 5.24. The correlation found from the best fitted power law curve can be shown as,

$$NTU = 17.56\ Re_w^{-0.33} \qquad (5\text{-}14)$$

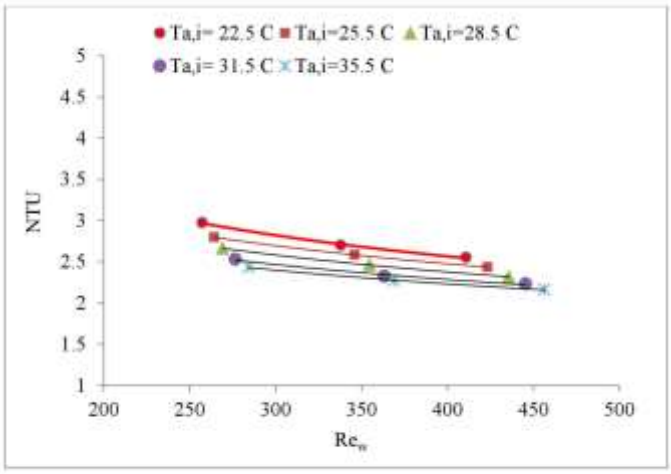

Figure 5.24 The effect of Re_w on NTU for different $T_{a,i}$

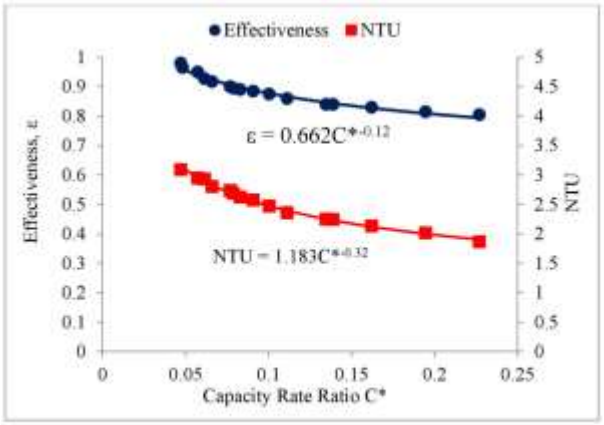

Figure 5.25 The effect of C* on ε and NTU

The Heat Capacity Rate Ratio (C*) Effect

The effect of the capacity rate ratio (C*) on ε and NTU is plotted in Figure 5.25, where generally ε increases with the increase in NTU. The increase in NTU values starts around 1.5 that corresponds to an effectiveness value close to 0.8. The correlations for both curves are as follows,

$$\varepsilon = 0.66\ C^{*-0.12} \qquad (5\text{-}15)$$

$$NTU = 1.18\ C^{*-0.32} \qquad (5\text{-}16)$$

NTU > 3 is not economically justifiable. The NTU values for this type of heat exchanger lie within the economical range which is 2 < NTU < 3.1. The plot also shows that both ε and NTU decrease when increasing C*, knowing that the range of C* varies between 0 < C* < 1. Effectiveness reaches its maximum value of 1 at C*=0 and a minimum value when C*=1. In this investigation, C* was found within 0.05 < C* < 0.23 which is lower than 1.

The -NTU relation is illustrated in Figure 5.26 where a power law curve fit initiates to be best curve fit.

$$\varepsilon = 0.63NTU^{0.37} \qquad (5\text{-}17)$$

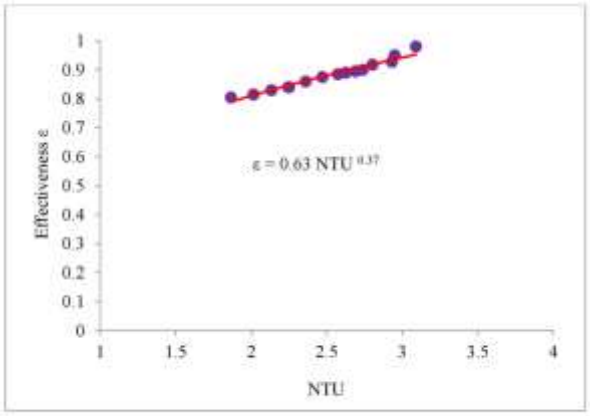

Figure 5.26 The effect of NTU on effectiveness

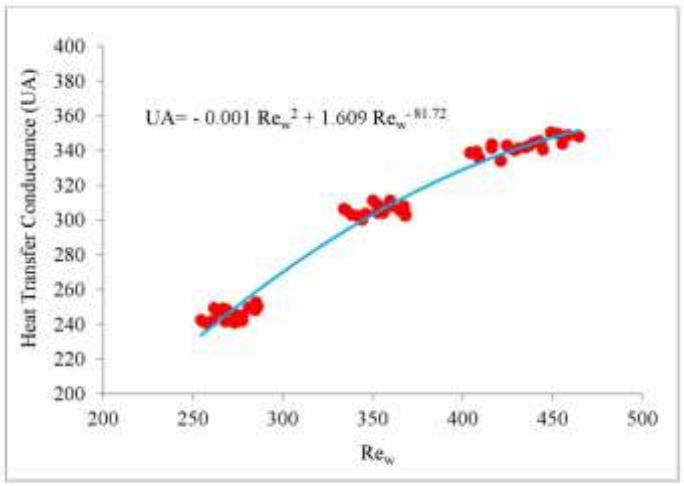

Figure 5.27 The effect of Re_w on heat transfer coefficient (UA)

Overall Heat Transfer Coefficient (UA)

The overall heat transfer coefficient (UA) shows how well the heat scatters in heat exchangers and represents the reciprocal of the total thermal resistance (R_{total}). It can be directly calculated from equation (3.40). The relationship between water Reynolds number and the overall heat transfer units (UA) is illustrated in Figure 5.27, UA increases with the increase in Rew for a specific air inlet temperature as well as with the increase of Ta,i for a particular value of Re_a.

In the current study, UA values varied from 240 UA 350. The correlation of UA- Re_w is obtained as,

$$UA = -0.001\ Re_w^{\,2} + 1.609\ Re_w^{\,-81.72} \qquad (5\text{-}18)$$

Axial Conduction Number (M)

A new non-dimensional number quantifying the axial conduction part in the walls is the axial conduction number (M). Heat transfer by conduction in the walls of mini–microchannels is quite multidimensional, which can become strongly non-uniform for low Reynolds numbers. Most of the heat flux is transferred to the fluid flow at the entrance of the mini–micro-channels,

Maranzana (2004). As a conclusion, the axial conduction in the walls of a mini–micro heat exchanger yields a loss of efficiency. An optimal wall conductivity that maximizes this efficiency exists, Maranzana (2004). Axial conduction number can be calculated from equation (3.19). Figure 5.28 illustrates Rew vs. the axial conduction number. It indicates that at lower Rew, the axial conduction number is higher which results in higher axial heat conduction. It also shows that by increasing Ta,i for a constant Rew, as M increases, the axial heat conduction increases as well. Axial heat conduction is significant when M get higher than M > 0.01. For the current study, the axial conduction number varied between 0.002 < M < 0.0033, which shows that the axial heat conduction doesn't have an influence on the heat transfer in the MICHX. Moreover, the trend shows that even for lower velocity, consequently lower Rew in MICHX, the axial heat conduction could not be taken into consideration because the M <<0.01.

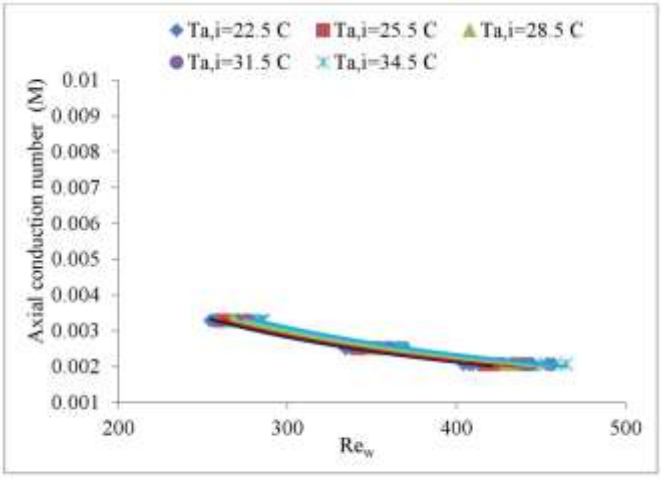

Figure 5.28 The effect of Re_w on M

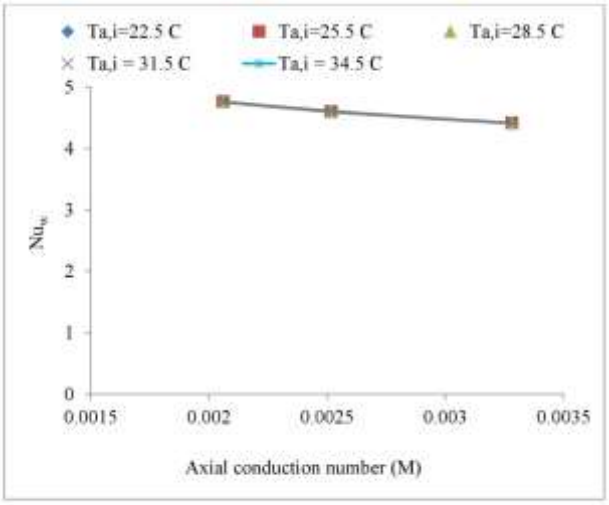

Figure 5.29 The effect of axial conduction number (M) on Nu_w

Distribution of ΔTs along the Channel Length

The distribution of temperature drop along the channel length for the water flow is illustrated in Fig. 5.30. The liquid temperature drops significantly in the first three slabs which indicate that most of the heat transfer occurs there. The heat transfer rate in the last two slabs is found to be less significant. According to this finding, eliminating the last two slabs from the MICHX will lead to:

- Reduce the size of the heat exchanger and save space.
- Decrease the pressure drop across the heat exchanger which decreases the required power.
- Reduced material and fabrication cost.

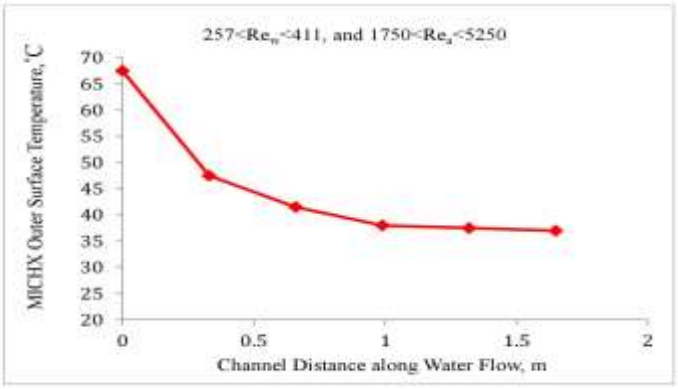

Figure 5.30 Temperature drop vs. channel length

VI. CONCLUSIONS & RECOMMENDATIONS

Summary and Conclusion

A thermal performance study is carried out to characterize the heat transfer in cross-flow MICHX with DI-water and air as the working fluids. This study investigates the effects of dimensionless parameters such as: Reynolds number (Re), and Nusselt number (Nu) for both fluids upon heat flow behaviour. The key parameters, such as heat transfer rates, NTU, Effectiveness, overall thermal resistance, axial heat conduction, and viscous dissipation are investigated. Empirical relationships are created between the heat transfer and key fluid-flow dimensionless parameters. Sixty distinct operating conditions are maintained in order to obtain these key Parameters. DI-water inlet temperature has been maintained constant at 75 ℃ all through the study, while air temperatures were varied at 22.5, 25.5, 28.5, 31.5, and 34.5 ℃. Three different DI water mass flow rates 0.022 Kg/s, 0.029 Kg/s, and 0.035 Kg/s were examined. For each mass flow rate, four air velocities: 6, 10, 14, and 18 m/s were applied. The following observations have been found from the current study:

1. The heat Balance (HB %) indicates the difference in rate of the heat released by DIwater and the heat gained by air to be less than 7%, which means that the MICHX has a negligible heat loss to the surrounding.
2. The results for Nu_a correlation found from the current study for air heating are compared to Dasgupta's results for air cooling. It is found that the heat transfer performance for air cooling and heating followed the same trend and slightly more enhanced for heating mode.
The correlations found in this study are:

$$Nu_a = 0.315\ Re_a^{0.373}\ Pr_a^{0.33}, \qquad \text{for } 1750 < Re_a < 5250,\ 0.71 \le Pr \le 0.72$$

or

$$Nu_a = 0.281\ Re_a^{0.373}, \qquad \text{for } 1750 < Re_a < 5250$$

The Pr for air is 0.71 which is incorporated into the constant 0.281.
3. The current study results for Nu_w correlation and air heating using DI-water are compared to Khan's results for 50% glycol-water mixture. Although the current predicted somewhat higher Nu_w, however, it agrees reasonably well with the result found by Khan et al. (2004).
The correlations found in this investigation are:

$$Nu_w = 1.2Re_w\ 0.17Pr_w 0.33, \qquad \text{for } 255 < Re_w < 411$$

4. The Reynolds number found to be the key factor affecting the heat transfer mechanism. The heat transfer rate increases with the increase of Re_a and Re_w in a power law relationship. The increase in Q when increasing Re_w is found larger compared to the increase in Q with the increase of Re_a.
5. Liquid heat transfer important factors such as; Nusselt number, heat transfer rate, convective heat transfer coefficient, normalized heat transfer rate, and LMTD are highly dependent on DI-water Reynolds number. The parameters increase with the increase in water Reynolds number in accordance to a power-law correlation.
6. The Dean number (De) in the channel curvature is higher than 11.6 which indicate an existence of a secondary flow in the bend. Thus, the serpentine plays a key role in developing a new velocity profile and boundary layer at the inlet of the proceeding slab which enhances the heat transfer. This effect is more prominent in the first three slabs compared to the last two slabs.
7. The Brinkman number is an important dimensionless number related to viscosity. The range of Br is found as 5.0E-9 < Br < 1.3E-8. This number is small in amount; it indicates that DI-water contribution to viscous dissipation is negligible.
8. Effectiveness ( ) and NTU increase with the increase in Rea in MICHX. However, they decrease with the increase in Rew, and heat capacity rate ratio (C*). Both factors make a power-law relationship with Rew, and C* as,

$$\varepsilon = 4.2\ Re_w^{0.26}$$

$$NTU = 16.79\ Re_w^{0.326}$$

$$\varepsilon = 1.27\ C^{*-0.3}$$

$$NTU = 0.64\ C^{*-0.158}$$

9. The NTU values varied from 2.25 < NTU < 2.75 and effectiveness varied from 82 %< ἐ <97%. Therefore, MICHX was operating nearly at its maximum thermal size.
10. Scale down multiport MICHX has superior capability to transfer heat between DI $_{water}$ and air due to the slab serpentine geometry. The flat heat transfer surface on both sides of each slab provide a better contact with the air stream as it eliminates the wake region formation at the back of the tubes in inline conventional heat exchangers. Adding to that, the flat surface makes the temperature distribution uniform on the air side resulting in a superior heat transfer rate for air heating and cooling.

Recommendations

The findings of the recent investigation in the field of heat transfer and fluid flow can contribute to future research in multiport cross flow MICHXs. Many challenges have been faced to collect the imperative information from the recent study; however substantial observation is still remained to be considered. The observation can be enhanced by using a wider range of operating conditions and conducting more experiments. Extended recommendations can also include:

1. Investigation of changing different heat exchanger core geometries and sizes, various fins size and shapes to check their effect on heat transfer and fluid flow characteristics.
2. Optimization of the channel diameter and its effect on the fluid flow and heat transfer characteristics.
3. Axial heat conduction in the wall and the liquid, particularly at low Nu and Re numbers, can be further examined.
4. The use of a thermal imaging device to study the heat and temperature distribution along the channels, in the serpentines, and on the air-side for the MICHX. Since the use of this device will provide the temperature distribution along the channel which is assumed constant for the current study. This will result in a better insight of the heat transfer and fluid flow.
5. Increase the capability of the system to include different operating conditions such as: fluid temperatures, flow rates, and more variation of air velocities to cover a wide range of applications.

VII. REFERENCES

[1] American Society of Mechanical Engineers. “Air Cooled Heat Exchangers” An American National Standard, Performance Test Code (PTC) 30-1991. ASME: NY, USA, 1991.

[2] Bahrami, M., Yovanovich, M., and J.R., Colham. “A Novel Solution for Pressure Drop in Singly Connected Microchannel of Arbitrary Cross Section” International Journal of Heat and Mass Transfer, 50:2492-2502, 2006.

[3] Bahrami, M., Tamayol, A., and P., Taheri. ”Slip-Flow Pressure Drop in Microchannels of General Cross Section” Transactions of the ASME 031201-8, Vol. 131, March 2009.

[4] Bier, W. “Manufacturing and Testing of Compact Micro Heat Exchangers with High Volumetric Heat Transfer Coefficients“ American Society of Mechanical Engineers, dynamic Systems and Control Division, DSC 19: 189-197, 1990.

[5] Bowman, R. A., Mueller, A. C., and W. M., Nagle. "Mean Temperature Difference in Design" Transactions of the ASME 62(1): 283-294, 1940.

[6] Cao, H., Chen, G. and Q., Yuan. “Thermal Performance Of Cross Flow Microchannel Heat Exchangers” Industrial Engineering Chemical Resource. 49(13): 6215-6220, 2010.

[7] Carrier. “Microchannel Technology - More Efficient, Compact, and Corrosion Resistant Technology for Air-Cooled Chiller Applications” Carrier Corporation, New York, USA, 2006.

[8] Celata, G. P., Morini, G.L., Marconi, V., McPhail, S.J., and G. Zummo. “Using Viscous Heating to Determine the Friction Factor in Microchannels an Experimental Validation” Experimental Thermal and Fluid Science, 30(8):725–731, 2006.